Algorithm for reconstruction of wind profile from turbulent intensity fluctuations of a scattered wave in a receiving telescope

D.A. Marakasov

Institute of Atmospheric Optics,
Siberian Branch of the Russian Academy of Sciences, Tomsk

Received August 6, 2007

The problem of reconstruction of the wind velocity profile from turbulent fluctuations of a laser beam scattered by a diffuse screen is considered. Equations are derived for the spatiotemporal correlation function of weak intensity fluctuations in a receiving telescope and its spectrum. The algorithm for reconstruction of the wind profile and direction is developed. Computer simulations confirm the efficiency of the algorithm developed.

Introduction

The problem of the wind velocity measurement from the spatiotemporal statistics of turbulent intensity fluctuations of an optical wave is of interest for a wide range of investigators. Measurement methods for the path-averaged transverse wind component were proposed and experimentally confirmed in Ref. 1 and references therein. In recent time, the ways to estimate the wind profile from the spatiotemporal correlation of intensity fluctuations of intersecting rays (SCIDAR),[2–6] which provide for reconstruction of the wind profile and the structure characteristic of the refractive index with a resolution up to several hundreds of meters, as well as approaches based on correlation-spectral analysis of intensity fluctuations[7–9] were proposed.

Analysis of intensity fluctuations of a wave scattered by the surface of an irradiated object also allows estimation both of the path-averaged wind velocity[10] and the wind profile.[11] Algorithm of the wind profile reconstruction from intensity fluctuations of the scattered radiation focused by an objective of a receiving device was developed,[12–14] based on the earlier approaches.[7–9] This algorithm allows reconstruction of the profile at the entire path with a spatial resolution of several tens of meters. However, since the image is scaled in a receiving system, the algorithm requires the use of a receiving device with a size of about 1 m, which is not always realizable in practice.

This paper generalizes the approach proposed in Ref. 14. This generalization allows the dimensions of the receiving device to be considerably reduced due to introduction of an additional lens (ocular). Equations for the spatiotemporal correlation function of intensity fluctuations and its spectrum are derived along with basic equations for determination of the value and direction of the transverse wind component. Results of numerical simulation confirming the efficiency of the proposed algorithm are presented.

1. Formulation of the problem and basic equations

Let laser source at the plane $x = 0$ irradiate a diffuse surface in the plane $x = L$. The scattered radiation in the source plane passes through an objective and an ocular of the receiving telescope, lying in the planes $x = 0$ and $x = -l_1$, respectively, and is recorded by a photodetector array (video camera) in the plane $x = -l_1 - l_2$. To simplify the procedure of the wind profile reconstruction, we assume that the receiving objective and the source are separated by some distance in the plane $x = 0$ (Fig. 1). As is shown in Ref. 13, this allows us to neglect correlation of the incident and reflected waves. Information about wind on the path between the source and the diffuse surface is obtained from two-dimensional intensity distributions in the recording plane by the correlation-spectral analysis.

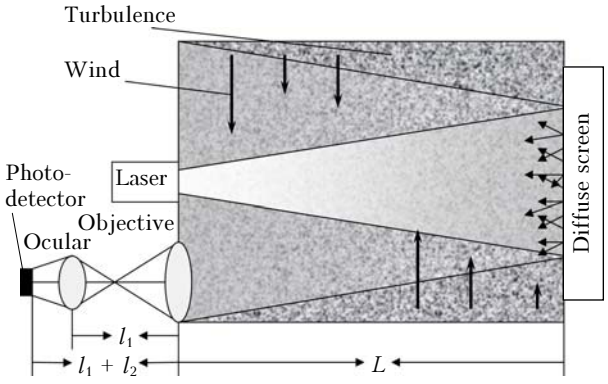

Fig. 1. Geometry of the problem.

When analyzing the spatiotemporal correlation function

$$K_I(\mathbf{R}, \rho; \tau) = \langle I(\mathbf{R} + \rho/2, 0)\, I(\mathbf{R} - \rho/2, \tau)\rangle - \\ - \langle I(\mathbf{R} + \rho/2, 0)\rangle \langle I(\mathbf{R} - \rho/2, \tau)\rangle, \quad (1)$$

where $I(\rho, \tau)$ is the wave intensity in the recording plane $x = -l_1 - l_2$ at the time τ, we assume that fluctuations of the reflection coefficient are independent of fluctuations of the air permittivity and the time scale of correlations of the reflection coefficient is smaller than the interval between frames. In Eq. (1) we can use the intensity values averaged over fluctuations of the reflection coefficient. For the regime of weak intensity fluctuations, the consideration can be restricted to the first significant term in the expansion of the correlation function (1) in a series in terms of intensity fluctuations[14]:

$$K_I(\mathbf{R},\rho;\tau) = \frac{16\pi^2}{k^4}\int d\mathbf{r}_{1,2}\left|A(\mathbf{r}_1)\,A(\mathbf{r}_2)\right|^2\left[I_{t0}\left(\mathbf{R}+\frac{\rho}{2},\mathbf{r}_1\right)\times\right.$$

$$\times I_{t0}\left(\mathbf{R}-\frac{\rho}{2},\mathbf{r}_2\right)K_{I_i}\left(\frac{\mathbf{r}_1+\mathbf{r}_2}{2},\mathbf{r}_1-\mathbf{r}_2;\tau\right)+I_{i0}(\mathbf{r}_1)I_{i0}(\mathbf{r}_2)\times$$

$$\left.\times K_{I_t}\left(\frac{\mathbf{r}_1+\mathbf{r}_2}{2},\mathbf{r}_1-\mathbf{r}_2;\mathbf{R},\rho;\tau\right)\right], \qquad (2)$$

where $k = 2\pi/\lambda$, λ is the wavelength; $A(\mathbf{r})$ is the amplitude of the scattering coefficient; $I_{i0}(\mathbf{r})$ and $I_{t0}(\rho, \mathbf{r})$ are intensities of the irradiating and telescopic beams in the plane of a reflector in the absence of permittivity fluctuations;

$$K_{I_i}\left(\frac{\mathbf{r}_1+\mathbf{r}_2}{2},\mathbf{r}_1-\mathbf{r}_2;\tau\right) =$$

$$= \langle I_i(\mathbf{r}_1;0)I_i(\mathbf{r}_2;\tau)\rangle - \langle I_i(\mathbf{r}_1)\rangle\langle I_i(\mathbf{r}_2)\rangle, \qquad (3)$$

$$K_{I_t}\left(\frac{\mathbf{r}_1+\mathbf{r}_2}{2},\mathbf{r}_1-\mathbf{r}_2;\mathbf{R},\rho;\tau\right) =$$

$$= \left\langle I_t\left(\mathbf{R}+\frac{\rho}{2},\mathbf{r}_1;0\right)I_t\left(\mathbf{R}-\frac{\rho}{2},\mathbf{r}_2;\tau\right)\right\rangle -$$

$$-\left\langle I_t\left(\mathbf{R}+\frac{\rho}{2},\mathbf{r}_1\right)\right\rangle\left\langle I_t\left(\mathbf{R}-\frac{\rho}{2},\mathbf{r}_2\right)\right\rangle \qquad (4)$$

are correlation functions of the intensities of the irradiating $I_i(\mathbf{r}, \tau)$ and telescopic $I_t(\rho, \mathbf{r}, \tau)$ beams, respectively.

For calculation of the correlation functions (3) and (4), it is convenient to introduce the functions

$$U_{i0}(\mathbf{r}) = \frac{k}{2\pi i L}\int d\rho_1 U_0(\rho_1)\exp\left\{\frac{ik}{2L}\rho_1^2 - \frac{ik}{L}\mathbf{r}\rho_1\right\}; \qquad (5)$$

$$U_{t0}(\mathbf{r}) = \frac{k}{2\pi i L}\int d\rho_2 h_t(\rho,\rho_2)\exp\left\{\frac{ik}{2L}\rho_2^2 - \frac{ik}{L}\mathbf{r}\rho_2\right\}, \qquad (6)$$

the squares of absolute values of which coincide with the intensities $I_{i0}(\mathbf{r})$ and $I_{t0}(\rho, \mathbf{r})$. Here $U_0(\rho)$ is the complex amplitude of the field created by the source in the plane $x = 0$; the function $h_t(\rho, \rho_2)$ has a meaning of the Green's function of the receiving device and determines the complex amplitude of the field induced at the point ρ_2 of the objective plane $x = +0$ by a point source lying at the point ρ of the recording plane $x = -l_1 - l_2$. We assume that the relative variance of intensity fluctuations is smaller than unity, and spatiotemporal variations of the permittivity field can be described using the Taylor hypothesis of frozen turbulence[15]:

$$\varepsilon_1(x, \rho; \tau) = \varepsilon_1[x, \rho - \mathbf{V}(x)\,\tau; 0], \qquad (7)$$

where $\mathbf{V}(x)$ is the wind component perpendicular to the direction of propagation. The averaging over permittivity fluctuations in Eqs. (3) and (4) is performed analogously to Ref. 14:

$$K_{I_i}\left(\frac{\mathbf{r}_1+\mathbf{r}_2}{2},\mathbf{r}_1-\mathbf{r}_2;\tau\right) = 2k^2L\int_0^1 d\xi\int d\boldsymbol{\kappa}\,C_n^2(L\xi)\Phi_n(\boldsymbol{\kappa})\times$$

$$\times\mathrm{Re}\left\{e^{i\boldsymbol{\kappa}(\mathbf{V}(\xi L)\tau+\xi\Delta)}U_{i0}\left(\mathbf{r}_1-\frac{L}{k}(1-\xi)\boldsymbol{\kappa}\right)U_{i0}^*(\mathbf{r}_1)\times\right.$$

$$\times\left[U_{i0}(\mathbf{r}_2)U_{i0}^*\left(\mathbf{r}_2-\frac{L}{k}(1-\xi)\boldsymbol{\kappa}\right)-\right.$$

$$\left.\left.-U_{i0}\left(\mathbf{r}_2+\frac{L}{k}(1-\xi)\boldsymbol{\kappa}\right)U_{i0}^*(\mathbf{r}_2)e^{i\xi(\xi-1)\kappa^2L/k}\right]\right\}, \qquad (8)$$

$$K_{I_t}\left(\frac{\mathbf{r}_1+\mathbf{r}_2}{2},\mathbf{r}_1-\mathbf{r}_2;\mathbf{R},\rho;\tau\right) = 2k^2L\int_0^1 d\xi\int d\boldsymbol{\kappa}\,C_n^2(L\xi)\Phi_n(\boldsymbol{\kappa})\times$$

$$\times\mathrm{Re}\left\{e^{i\boldsymbol{\kappa}(\mathbf{V}(\xi L)\tau+\xi\Delta)}U_{t0}\left(\mathbf{R}+\frac{\rho}{2},\mathbf{r}_1-\frac{L}{k}(1-\xi)\boldsymbol{\kappa}\right)\times\right.$$

$$\times U_{t0}^*\left(\mathbf{R}+\frac{\rho}{2},\mathbf{r}_1\right)\left[U_{t0}\left(\mathbf{R}-\frac{\rho}{2},\mathbf{r}_2\right)\times\right.$$

$$\times U_{t0}^*\left(\mathbf{R}-\frac{\rho}{2},\mathbf{r}_2-\frac{L}{k}(1-\xi)\boldsymbol{\kappa}\right)-U_{t0}\left(\mathbf{R}-\frac{\rho}{2},\mathbf{r}_2+\frac{L}{k}(1-\xi)\boldsymbol{\kappa}\right)\times$$

$$\left.\left.\times U_{t0}^*\left(\mathbf{R}-\frac{\rho}{2},\mathbf{r}_2\right)e^{i\xi(\xi-1)\kappa^2L/k}\right]\right\}, \qquad (9)$$

where $\Delta = \mathbf{r}_1 - \mathbf{r}_2$; $C_n^2(x)$ is the structural characteristic of the atmospheric turbulence; $\Phi_n(\boldsymbol{\kappa})$ is the three-dimensional spectrum of the refractive index fluctuations.[16]

The function (5) entering into Eq. (8) is calculated on the assumption that the initial source field is Gaussian:

$$U_0(\rho) = U_0\exp\left\{-\frac{\rho^2}{2a_0^2} - \frac{ik}{2F_0}\rho^2\right\}, \qquad (10)$$

where a_0 and F_0 are the beam radius and the wavefront curvature radius, respectively; U_0 is the amplitude of the field on the optical axis. Substitution of Eq. (10) in Eq. (5) yields

$$U_{i0}(\mathbf{r}) = \frac{ikU_0}{z_iL}\exp\left\{\frac{k^2r^2}{2z_iL^2}\right\},\ z_i = -\frac{1}{a_0^2} + ik\left(\frac{1}{L} - \frac{1}{F_0}\right). \qquad (11)$$

We introduce the Green's function for the objective ($j = 1$) and the ocular ($j = 2$) [Ref. 15]:

$$h_j(l_j,\rho,\rho') = \frac{k}{2\pi i l_j}\exp\left\{-\frac{\rho'^2}{2a_{tj}^2} - \frac{ik}{2F_{tj}}\rho'^2 + \frac{ik}{2l_j}(\rho-\rho')^2\right\}, \qquad (12)$$

where the Gaussian approximation is taken for the transmission function of the lenses; $F_{t1,2}$ are the focal lengths of the lenses; $a_{t1,2}$ are the effective radii. The function $h_t(\rho, \rho_2)$ can be expressed through (12) as follows:

$$h_t(\rho,\rho_2) = \int d\rho_1 h_1(l_1,\rho_1,\rho_2) h_2(l_2,\rho,\rho_1). \quad (13)$$

Substitution of Eq. (13) in Eq. (6) allows the integral over the objective surface to be calculated:

$$U_{t0}(\rho,\mathbf{r}) = \frac{ik^3}{2\pi L l_1 l_2 z_t z_{t0}} \times$$

$$\times \exp\left\{\frac{ik}{2l_2}\left(1-\frac{ik}{z_{t0}l_2}\right)\rho^2 + \frac{k^2}{2z_t L^2}\left(\mathbf{r} - \frac{ikL}{z_{t0}l_1 l_2}\rho\right)^2\right\}, \quad (14)$$

$$z_{t0} = \frac{1}{a_{t2}^2} + ik\left(\frac{1}{l_1}+\frac{1}{l_2}-\frac{1}{F_{t2}}\right),$$

$$z_t = \frac{1}{a_{t1}^2} + ik\left(\frac{1}{l_1}+\frac{1}{L}-\frac{1}{F_{t1}}\right) + \frac{k^2}{l_1^2 z_{t0}}. \quad (15)$$

The screen image in the recording plane contracts according to the scaling coefficient

$$m = \frac{L l_1 l_2}{k^3 a_{td}^2 \operatorname{Im}\left(\frac{1}{z_{t0} z_t}\right)}, \quad (16)$$

where $a_{td}^2 = L^2|z_t|^2/(k^2 \operatorname{Re} z_t)$ is the square radius of the telescopic beam on the screen, which in the absence of ocular ($l_2 \to 0$, $F_{t2} \to \infty$, $a_{t2} \to \infty$) transforms into the ratio of the distance between the objective and detector to the path length.[14] Since to reconstruct the wind profile, it is necessary to resolve parts of the diffuse screen surface with the scales comparable with the Fresnel radius $\sqrt{L/k}$, the minimal dimensions of the receiver, for example, for a 1-km long path appear to be ~1 m. With the proper selection of the ocular parameters, the contraction coefficient and, consequently, the telescope dimensions can be decreased many times.

Calculate integrals over the reflector surface in Eq. (2) taking into account Eqs. (8), (9) and (11), (14) and assuming the exponential amplitude of the reflection coefficient:

$$A(\mathbf{r}) = A_0 \exp\left\{-\frac{r^2}{2a_r^2}\right\}, \quad (17)$$

where A_0 is the amplitude at the center of the diffuse reflector; a_r is the effective radius of the reflector. As a result, we obtain the equation for the correlation function of intensity in the recording plane

$$K_I(\mathbf{R},\rho;\tau) = K_0 \exp\left\{-\frac{2\mathbf{R}^2 + \rho^2/2}{a^2}\right\} \times$$

$$\times \int_0^1 d\xi \int d\boldsymbol{\kappa}\, C_n^2(L\xi)\Phi_n(\boldsymbol{\kappa}) \times$$

$$\times \operatorname{Re}\left\{e^{i\kappa \mathbf{V}(\xi L)\tau} \sum_{n=1}^{2}\left[\exp(-\operatorname{Re}\beta_n \kappa^2 - 2\operatorname{Re}\gamma_n \mathbf{R}\boldsymbol{\kappa} + \right.\right.$$

$$\left.\left. + i \operatorname{Im}\gamma_n \rho\boldsymbol{\kappa}) - \exp(-\beta_n \kappa^2 + \gamma_n \rho\boldsymbol{\kappa})\right]\right\}, \quad (18)$$

which differs from the correlation function of turbulent intensity fluctuations of the scattered wave behind the lens[14] only by the values of parameters

$$K_0 = \frac{2L}{k^2}\left(\frac{k^4 a_s A_0 U_0}{l_1 l_2 L^2 |z_i z_{t0} z_t|}\right)^4; \quad (19)$$

$$\beta_{1,2} = \left(i\xi - \frac{k}{L z_{i,t}}(1-\xi)\right) \times$$

$$\times \left\{i\xi - \frac{k}{L z_{i,t}}\left(1 - \frac{2L^2 z_{i,t}}{k^2 a_s^2}\right)(1-\xi)\right\}; \quad (20)$$

$$\gamma_1 = -\frac{a_s^2}{m a_{td}^2}\left(i\xi - \frac{k}{L z_i}(1-\xi)\right),$$

$$\gamma_2 = \frac{ik^2(1-\xi)}{l_1 l_2 z_{t0} z_t} - \frac{a_s^2}{m a_{td}^2}\left(i\xi - \frac{k}{L z_t}(1-\xi)\right); \quad (21)$$

$$a_s = \left(a_r^{-2} + a_{td}^{-2} + \frac{k^2}{L^2 a_0^2 |z_i|^2}\right)^{1/2},$$

$$a = \left[\frac{k^2}{l_2^2}\operatorname{Re}\left(\frac{k^2}{l_1^2 z_{t0}^2 z_t} - \frac{1}{z_{t0}}\right) - \frac{a_s^2}{m^2 a_{td}^4}\right]^{1/2}. \quad (22)$$

2. Algorithm for wind profile reconstruction

To reconstruct the wind profile, we pass, as in Ref. 14, to the Fourier transform of the correlation function (18) normalized to the Kolmogorov spectrum of fluctuations of the refractive index $\Phi_n(\boldsymbol{\kappa}) = 0.033\kappa^{-11/3}$:

$$g_i(\alpha,q) = \frac{q a^{10/3}}{2^{20/3}\pi^5 K_0 \Phi_n(\mathbf{q})} \times$$

$$\times \int d\mathbf{R}\, d\rho\, d\tau K_I(R,\rho,\tau) \exp[i(\omega\tau + q\mathbf{e}_i\rho)], \quad (23)$$

where the vector of spatial frequency is directed along one of coordinate axes $\mathbf{q} = q\mathbf{e}_i$; $\mathbf{V}(x)\mathbf{e}_i = V_i(x)$ is the projection of velocity onto this axis; $\alpha = \omega/q$. As it follows from the analysis in Refs. 9 and 14, each point ξ of the path contributes significantly to the spectrum of intensity fluctuations only in the vicinity of two (the number of terms in the series in Eq. (18)) rays $\alpha = \text{const}$. Introduction of an auxiliary function

$$f_i(\alpha,p) = 4\int_0^\infty g_i(\alpha,q) e^{ipq^2} q\, dq =$$

$$= \int_0^1 d\xi\, C_n^2(L\xi) \sum_{n=1}^{2}\left|\frac{\operatorname{Im}\gamma_n}{\operatorname{Re}\eta_n}\right|^{11/3} \delta\left(\alpha - \frac{a^2 \operatorname{Im}\gamma_n}{2\operatorname{Re}\eta_n} V_i(\xi L)\right) \times$$

$$\times\left\{\frac{2/\mathrm{Re}\,\eta_n}{\frac{a^2}{2}\left(1\frac{a^2(\mathrm{Im}\,\gamma_n)^2}{2\mathrm{Re}\,\eta_n}\right)-ip}-\frac{1/\eta_n}{\frac{a^2}{2}\left(1+\frac{a^2\gamma_n^2}{2\eta_n}\right)-ip}-\right.$$

$$\left.-\frac{1/\eta_n^*}{\frac{a^2}{2}\left(1+\frac{a^2\gamma_n^{*2}}{2\eta_n^*}\right)-ip}\right\}, \qquad (24)$$

where $\eta_n = \beta_n - (a^2\gamma_n^2/2)$, allows us to assign two peaks of the absolute value of $|f_i(\alpha, p)|$ with the coordinates

$$p_n \approx \frac{a^4}{4}\mathrm{Im}\left(\frac{\gamma_n^2}{\eta_n}\right), \quad \alpha_n = \frac{a^2\,\mathrm{Im}\,\gamma_n}{2\mathrm{Re}\,\eta_n}V_i(\xi L) \qquad (25)$$

lying in the area $p > 0$ to every point of the path. Thus, finding the peaks of $|f_i(\alpha, p)|$ and solving equations (25) for ξ and $V_i(\xi L)$, we can reconstruct the profile of the wind velocity projection $V_i(x)$ on the axis $\mathbf{e}_i$. Reconstructing another component of the transverse wind velocity in the same way, we find the wind profile.

3. Reconstruction of the wind profile by numerical experiments

To check the efficiency of the proposed algorithm, we numerically simulated the laser beam propagation in the turbulent atmosphere and its scattering on a diffuse screen. The intensity of the wave scattered by the diffuse screen was calculated using the approximate algorithm.[17] Propagation of the irradiating beam through the atmosphere was simulated by the algorithm developed in Ref. 18. Atmospheric inhomogeneities were simulated through disturbance of the propagating wave by equidistant random phase screens with the Kolmogorov spectrum of phase fluctuations. Parameters of the screens and their number were selected so that they ensured the needed accuracy of simulation and the regime of weak fluctuations.

The wind on the path was simulated by transverse displacements of the positions of phase screens with time to the distance $\mathbf{V}(x)\tau$. The obtained realizations of intensity in the photodetector plane were used to calculate the Fourier-transform spectrum of the correlation function (23), which was processed by Eq. (24), and then the wind profile was determined from coordinates of peaks of the functions $|f_i(\alpha, p)|$.

In the numerical experiment, the following values of the simulation parameters were specified: the path length L = 1000 m, the wavelength λ = 0.5 μm, $C_n^2 = 1 \cdot 10^{-16}$ m$^{-2/3}$, objective parameters F_{t1} = 43.7 cm, a_{t1} = 5 cm, ocular parameters F_{t2} = 2.5 cm, a_{t2} = 5 cm, distance between the lenses l_1 = 50 cm. The photodetector was located in the sharp-image plane. The laser beam was taken convergent with a focal length of 2 km and the initial radius a_0 = 5 cm. Beam propagation in the atmosphere ($0 \le x \le L$) was simulated on a 512×512 spatial grid with a step of 1.5 mm. In the photodetector plane, the computational grid was scaled in so way that its step was equal 13.5 μm. The spectrum was estimated from twenty realizations of intensity distributions with duration equal to 256 readings in time with a lag of 1.5 ms. The results of calculation of the spatiotemporal spectrum (23) are shown in Fig. 2 in the logarithmic scale.

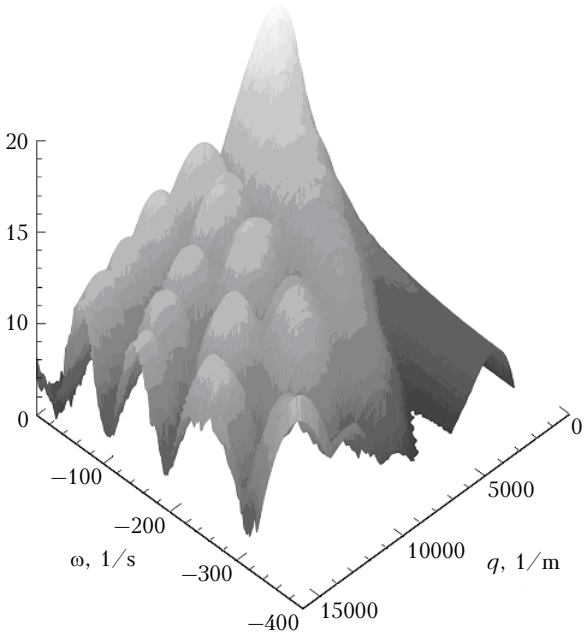

Fig. 2. Spatiotemporal spectrum of intensity fluctuations in the sharp-image plane.

Every phase screen is shown as a ray, along which the spectral density takes far higher values than in its vicinity. Figure 3 shows the results of reconstruction of wind profiles. Initial profiles are shown by the solid curve, while the reconstructed ones are shown by the dashed curve. Along the entire path, the wind profiles are reconstructed at an error not exceeding 40 m for the coordinate and 0.1 m/s for the speed.

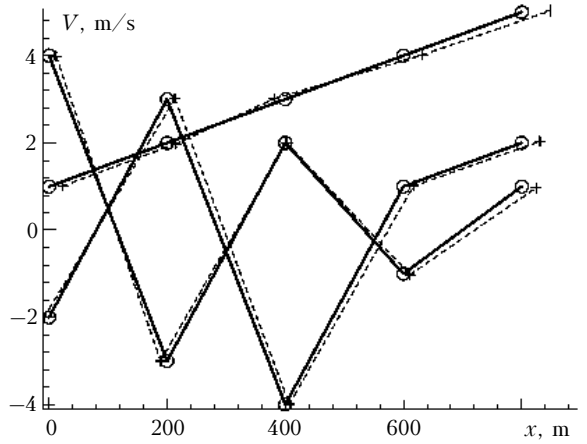

Fig. 3. Initial wind profiles (solid curves, positions of the screens are marked by circles) and profiles reconstructed from intensity fluctuations in the sharp-image plane (dashed curves).

The results of the numerical experiment demonstrate that the proposed algorithm allows the wind profile to be reconstructed from turbulent intensity fluctuations of laser radiation scattered by a diffuse screen in the sharp-image plane of the receiving telescope.

Conclusions

In this paper, we have considered the problem of the wind profile reconstruction from intensity fluctuations of radiation scattered by a diffuse screen in the turbulent atmosphere. It has been shown that under the conditions of weak optical turbulence every point of a path represents in the spatiotemporal intensity spectrum as two bands originating from the origin of coordinates, whose tilt is proportional to the wind speed at this point. The algorithm has been developed for reconstruction of the wind profile from the spatiotemporal spectrum of intensity fluctuations in the sharp-image plane.

The efficiency of the algorithm was confirmed by the results of numerical experiments on reconstruction of the wind speed and direction from computer-simulated random realizations of three-dimensional intensity distributions of laser radiation scattered by a diffuse screen.

It has been found that the use of a telescopic unit in the receiving system does not worsen the accuracy of reconstruction of the wind profile and allows the dimensions of the receiving device to be reduced to several tens of centimeters.

Acknowledgements

The author is grateful to V.A. Banakh and M.A. Vorontsov for initiation of this work and useful criticism.

The study was supported in part by the Technical Research Institute (USA) (Grant W911NF-05-1-0552) and Russian Foundation for Basic Research (Grants No. 06–05–64445 and No. 06–05–96951-reg).

References

1. T.-I. Wang, G.R. Ochs, and S. Lawrence, Appl. Opt. **20**, No. 23, 4073–4081 (1981).
2. R. Johnston, C. Dainty, N. Wooder, and R. Lane, Appl. Opt. **41**, No. 32, 6768–6772 (2002).
3. V.A. Kluckers, N.J. Wooder, T.W. Nicholls, M.J. Adcock, I. Munro, and J.C. Dainty, Astron. and Astrophys. Suppl. Ser. **130**, No. 1, 141–155 (1998).
4. J.-L. Prieur, R. Avila, G. Daigne, and J. Vernin, Publ. Astron. Soc. Pacif. **116**, No. 822, 778–789 (2004).
5. R. Avila, E. Carrasco, F. Ibanez, J. Vernin, J.-L. Prieur, and D.X. Cruz, Publ. Astron. Soc. Pacif. **118**, 503–515 (2006).
6. B. Garcia-Lorenzo and J.J. Fuensalida, Mon. Not. Roy. Astron. Soc. **372**, 1483–1495 (2006).
7. V.A. Banakh and D.A. Marakasov, Opt. Lett. **32**, No. 15, 2236–2238 (2007).
8. V.A. Banakh and D.A. Marakasov, J. Opt. Soc. Am. A **24**, No. 10, 3245–3254 (2007).
9. D.A. Marakasov, Quant. Electron. (2008) (in press).
10. S.F. Clifford, G.R. Ochs, and T.-I. Wang, Appl. Opt. **14**, 2844–2850 (1975).
11. V.A. Banakh and D.A. Marakasov, Quant. Electron. (2008) (in press).
12. V.A. Banakh, M.A. Vorontsov, and D.A. Marakasov, Quant. Electron. (2008) (in press).
13. V.A. Banakh, D.A. Marakasov, and M.A. Vorontsov, Appl. Opt. (2008) (in press).
14. V.A. Banakh and D.A. Marakasov, Quant. Electron. (2008) (in press).
15. H.A. Panofsky and J.A. Dutton, *Atmospheric Turbulence: Models and Methods for Engineering Applications* (A Wiley Interscience Publications, New York–Singapore, 1983), 397 pp.
16. V.I. Tatarsky, *Wave Propagation in a Turbulent Medium* (Dover, New York, 1961).
17. V.A. Banakh, Atmos. Oceanic Opt. **20**, No. 4, 271–274 (2007).
18. V.A. Banakh and A.V. Falits, Proc. SPIE **4678**, 132–143 (2001).